Significant stiffness reduction at ferroelectric domain boundary evaluated by ultrasonic atomic force microscopy

doi: 10.1063/1.2012537

Significant stiffness reduction at ferroelectric domain boundary evaluated by ultrasonic atomic force microscopy

T. Tsuji,[a] S. Saito, K. Fukuda, and K. Yamanaka
Department of Material Processing, Graduate School of Engineering, Tohoku University, 6-6-02 Aoba, Sendai 980-8579, Japan

H. Ogiso and J. Akedo
Advanced Integration Process Group, National Institute of Advanced Science and Technology, 1-2-1 Namiki, Tsukuba, Ibaraki 305-8564, Japan

Y. Kawakami
NEC Tokin Cooperation, 6-7-1, Koriyama, Sendai 982-8510, Japan

(Received 15 March 2005; accepted 12 July 2005; published online 10 August 2005)

Two-dimensional resonance frequency mapping in the ultrasonic atomic force microscopy was applied to the investigation of the ferroelectric domain structure in lead zirconate titanate ceramics. This method can visualize the stiffness anisotropy due to the differently oriented domains. Moreover, the significant stiffness reduction at the ferroelectric domain boundary was discovered. The disorder of the lattice, the ability of the switching of the domain, and the reduction of the piezoelectric stiffening are possible explanations. The implication of this work is the characterization of novel functional materials on nanoscale and the nondestructive evaluation of the microelectromechanical systems and nanotechnology devices. © *2005 American Institute of Physics*. [DOI: 10.1063/1.2012537]

The development of ferroelectric materials and devices has required the better understanding of not only the ferroelectric domain but also the ferroelectric domain boundary (DB) called domain wall. For example, the movement of ferroelectric and ferroelastic DB significantly enhanced the piezoelectric coefficient of the ferroelectric thin film.[1] In the engineering domain configuration of ferroelectric single crystals, the piezoelectric property depended on the fineness of the domain size.[2] One of the origins of the polarization fatigue in ferroelectric thin film is the pinning of the movement of the ferroelectric DB (Ref. 3).

The width of the DB was attributed in the order of 1–10 nm (Ref. 4), which has been studied by several methods such as transmission electron microscopy, scanning nonlinear dielectric microscopy (SNDM), and atomic force microscopy.[5–7] Although SNDM may provide dielectric information, we believe that the mechanical information is also important because the piezoelectric deformation and the polarization switching are related to the mechanical behavior of the domain and the DB.

Ultrasonic atomic force microscopy (UAFM) has been developed as the stiffness evaluation method on nanoscale (Refs. 8–13). Recently, we reported evidence of the reduction of the stiffness at the ferroelectric DB in a lead zirconate titanate [$Pb(Zr_x,Ti_{1-x})O_3$, PZT] ceramic.[12] However, the quantitative discussion required the two-dimensional (2D) mapping of the resonance frequency that may be realized by the resonance frequency tracking system.[11] In this study, we observed ferroelectric domains in PZT ceramics by the 2D mapping of the resonance frequency.

The detailed operation of the resonance frequency tracking system was reported in the Ref. 11. For imaging the ferroelectric domains, the piezoresponse force microscopy (PFM) was used.[14] Commercially available bulk PZT ceramics were investigated (sample 1: NEC Tokin Cooperation N-21, sample 2: Fuji Ceramics Cooperation C-82) (Refs. 15 and 16). Sample 1 was an unpoled material. Because sample 2 was a poled material, it was annealed in order to obtain random domain configuration. These were lapped by diamond slurry and polished by colloidal silica slurry and alumina paste for samples 1 and 2, respectively. They were glued to sample holders with silver paste. We used an Au coated and a chemical vapor deposition diamond film coated Si cantilever for samples 1 and 2, respectively, purchased from Nanosensor.[17] We performed the experiments in ambient air at 23 °C with the relative humidity in the range of 40–60 %.

First, we show the applicability of the UAFM to the stiffness evaluation of the PZT. Figure 1(a) shows a contact AFM topography of an area of sample 1. Figure 1(b) shows a PFM image of the same area as Fig. 1(a) representing the phase shift of the deflection vibration to the ac voltage applied between the tip and the bottom electrode (PFM image). The frequency and amplitude of the ac voltage were 4 kHz and 2.5 V, respectively. There was a stripe pattern with a period of 250 nm representing differently oriented domains. It may be 90° domain structure.[18] Figure 1(c) shows a UAFM image representing the resonance frequency at the third deflection mode (UAFM image). The darker color represents higher resonance frequency, indicating higher contact stiffness. The stripe pattern in the UAFM image was related to the domains. As a result, it was demonstrated that the UAFM can evaluate the different elasticity due to the differently oriented domains of PZT.

After confirming the applicability of the UAFM to PZT, we now applied it to the evaluation of the stiffness at the DB (Ref. 12). Figure 2(a) shows a topography of an area of sample 2 with the load F of 1200 nN. Figure 2(b) shows a PFM image of the same area where the applied ac voltage

[a]Electronic mail: t-tsuji@material.tohoku.ac.jp

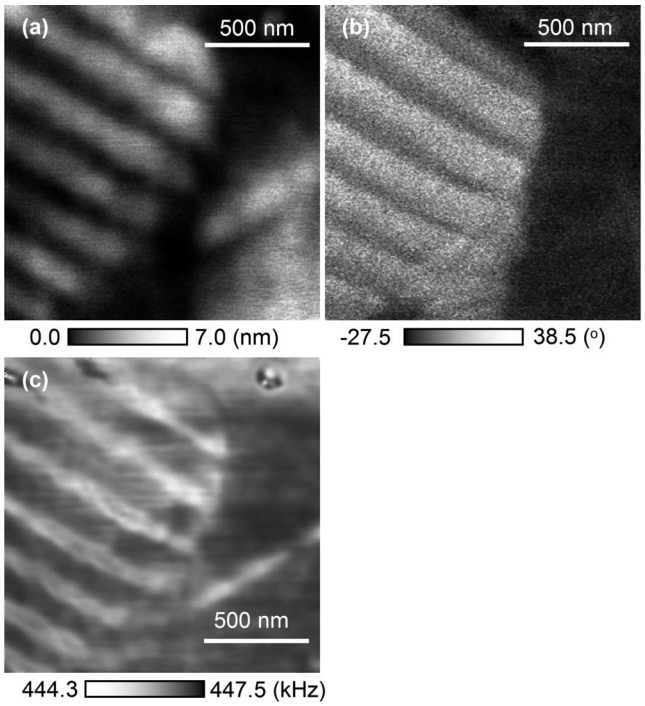

FIG. 1. Images of 90° domain in PZT ceramic (sample 1). (a) Topography, (b) PFM phase-shift image, and (c) UAFM resonance frequency image at the third deflection mode.

was the same as that in Fig. 1(b). Because uniformly bright and dark regions represent the ferroelectric domains, the boundaries between them represent the DBs. It may be 180° DBs because of the wavy shape.[18] Although the phase difference was much less than 180°, it may be explained by the integral piezoelectric response due to randomly polarized grains stacked in the normal to the surface and the capacitive

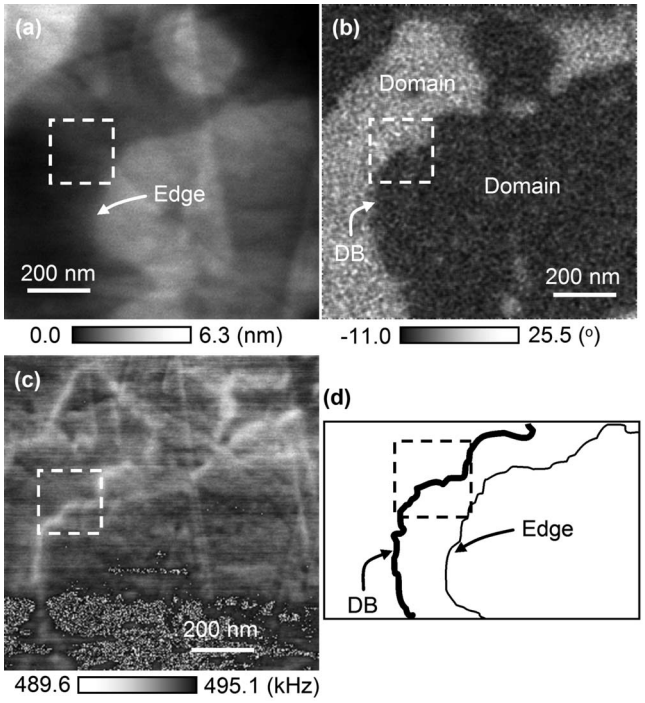

FIG. 2. Image of 180° domain in PZT ceramic (sample 2). (a) Topography, (b) PFM phase-shift image, and (c) UAFM resonance frequency image at the second deflection mode. (d) Schematic illustration of the relation between the configurations of the DB and the edge.

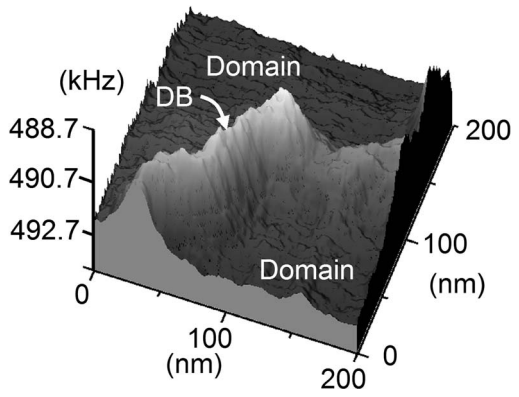

FIG. 3. Detailed UAFM image of ferroelectric DB.

force between the cantilever and the bottom electrode.[19,20] Figure 2(c) shows a UAFM image at the second deflection mode. There were stringlike structures showing lower resonance frequency. When we compare the same area surrounded by the dotted squares shown in Fig. 2, we note that the stringlike structures observed in Fig. 2(c) corresponded to the DBs observed in the PFM image, Fig. 2(b). At the same time, it does not correspond to the edge of the surface relief because the edge is out of the zone surrounded by the dotted square in Fig. 2(a). The relation between the DB and the edge is illustrated in Fig. 2(d). Therefore, it was verified that the stringlike structures were the DBs and not topographic artifacts. Figure 3 shows a bird's-eye view of the zone surrounded by the dotted square shown in Fig. 2(c). The apparent half width of the DB was in the range of 20–30 nm, which was widened due to finite contact area.

In order to obtain insight into the nature of the DB based on the above observation, we analyzed the stiffness on the DB. The resonance frequency $f=492.7$ kHz within the domain gives the contact stiffness $s_v=1305$ N/m, using cantilever vibration theory.[8] When the load F, the Young's modulus at the domain E_D, and the Poisson's ratio ν are 1200 nN, 117 GPa, and 0.34, respectively,[21] the tip radius R and the contact radius a are 55.1 and 8.72 nm, respectively, using Hertzian contact theory.[22] When F,R,a are identical within the image, $f=489.7$ kHz on the DB gives the averaged Young's modulus $\bar{E}=103$ GPa.

In order to evaluate the contribution of the Young's modulus of the DB, E_{DB} to the $\bar{E}$, we approximate the application of the stress in the experiment to that in the unidirectional fiber-reinforced composite materials and apply the linear mixture law of the Young's modulus.[23] The averaged modulus $\bar{E}$ is expressed by

$$\bar{E}=(1-R_{DB})E_D+R_{DB}E_{DB}, \tag{1}$$

where E_D and E_{DB} are the Young's moduli of the domain and the DB and R_{DB} are the area ratio of the DB to the total contact, respectively. The R_{DB} is expressed by

$$R_{DB}=\frac{2}{\pi}\left\{\frac{w}{a}\sqrt{1-\left(\frac{w}{a}\right)^2}+\frac{\pi}{2}-\arccos\frac{w}{a}\right\}, \tag{2}$$

where w is the half width of the DB. We estimated the stiffness of the DB normalized by that of the domain, E_{DW}/E_D (Ref. 24), for four different values of w (Ref. 25) as listed in Table I. As a result, we discovered that the stiffness at the DB is much lower than that of the domain when we assume

TABLE I. Variation in the stiffness of the DB normalized by that of domain, E_{DB}/E_D, depending on the half width of the DB, w.

w (nm)	1	2	5	8.72
E_{DB}/E_D	0.179	0.587	0.826	0.880

that the width of the DB is smaller than the contact radius. As shown in Table I, if w is 2 nm, E_{DW}/E_D is as low as 0.587.

Finally, we discuss possible explanations of this finding. (i) The disorder of the lattice at the DB; the imperfection of the crystal may reduce the stiffness. (ii) The ability of the switching of the domain; the switching accompanies the movement of the DB. It may be facilitated by the reduction of the stiffness at the DB because the polarization of the domain is constrained by the minimum state of the sum of the strain energy and the electrostatic energy. Therefore, the ability of the switching of the domain may reduce the stiffness. (iii) The reduction of the piezoelectric stiffening; when the polarization charge is not compensated during the application of the stress, the stiffness is enhanced because of the depolarization field (piezoelectric stiffening).[26] In the experiment of the UAFM, the polarization on the domain may lead to the piezoelectric stiffening, because the small contact area cannot compensate all polarization charge over the domain. On the other hand, because the spontaneous polarization of the lattice is rotated at the DB, the average polarization on the DB is smaller than that on the domain. As a result, the piezoelectric stiffening on the DB is smaller than that on the domain. Therefore, the reduction of the piezoelectric stiffening may reduce the stiffness.

We estimate the order of the reduction in the case of (iii), using the variation in stiffness coefficient c between the electrical conditions of the constant electric field and the constant electric displacement, represented by the superscripts E and D, respectively.[26] The ratio of stiffness coefficients is expressed by

$$\frac{c^E}{c^D} = 1 - k^2, \tag{3}$$

where k represents the electromechanical coupling coefficient in the poling direction. When we use the coupling coefficient,[16] c_{33}^E/c_{33}^D becomes 0.44 that is consistent with the result, E_{DB}/E_D.

In summary, we performed the evaluation of the ferroelectric domain boundary in PZT ceramics, using the resonance frequency image in the UAFM. After confirming the applicability of the UAFM to PZT by evaluating the stiffness anisotropy due to the differently oriented domains, we discovered a significant reduction of the stiffness at the DB. The disorder of the lattice, the ability of the switching of the domain, and the reduction of the piezoelectric stiffening are possible explanations. This phenomenon may be related to the enhanced piezoelectric properties. This evaluation method may provide the information of the polarization fatigue of ferroelectric thin films.[3] The implication of this work is the characterization of novel functional materials on nanoscale and the nondestructive evaluation of the microelectromechanical systems and nanotechnology devices.

This work was supported by the Japan Society for the Promotion of Science for Young Scientists, and by a Grant in Aid for Science Research (Nos. 13450017 and 15656179) from the Ministry of Education, Culture, Sports, Science and Technology.

[1] V. Nagarajan, A. Roytburd, A. Stanishevsky, S. Prasertchoung, T. Zhao, L. Chen, J. Melngailis, O. Auciello, and R. Ramesh, Nat. Mater. **2**, 43 (2002).
[2] S. Wada, H. Kakemoto, and T. Tsurumi, Materials Transactions **45**, 178 (2004).
[3] A. K. Tagantsev, I. Stolichnov, E. L. Colla, and N. Setter, J. Appl. Phys. **90**, 1387 (2001).
[4] M. E. Lines and A. M. Glass, *Principle and Applications of Ferroelectrics and Related Materials* (Clarendon, Oxford, 1977), p. 100.
[5] S. Stemmer, S. K. Streiffer, F. Ernst, and M. Ruhle, Philos. Mag. A **71**, 713 (1995).
[6] K. Matsuura, Y. Cho, and R. Ramesh, Appl. Phys. Lett. **83**, 2650 (2003).
[7] D. Shilo, G. Ravichandran, and K. Bhattacharya, Nat. Mater. **3**, 453 (2004).
[8] K. Yamanaka and S. Nakano, Jpn. J. Appl. Phys., Part 1 **35**, 3787 (1996).
[9] K. Yamanaka, A. Noguch, T. Tsuji, T. Koike, and T. Goto, Surf. Interface Anal. **27**, 600 (1999).
[10] K. Yamanaka, A. Noguchi, T. Tsuji, T. Koike, and T. Mihara, Rev. Sci. Instrum. **71**, 2403 (2000).
[11] K. Yamanaka, Y. Maruyama, T. Tsuji, and K. Nakamoto, Appl. Phys. Lett. **78**, 1939 (2001).
[12] T. Tsuji, H. Ogiso, J. Akedo, S. Saito, K. Fukuda, and K. Yamanaka, Jpn. J. Appl. Phys., Part 1 **43**, 2907 (2004).
[13] U. Rabe, M. Kopycinska, S. Hirsekorn, J. Munoz Saldana, G. A. Schneider, and W. Arnold, J. Phys. D **35**, 2621 (2002).
[14] A. Gruverman, *Nanoscale Characterization of Ferroelectric Materials*, edited by M. Alexe and A. Gruverman (Springer, New York, 2004).
[15] Data sheet of NEC Tokin Cooperation (Sendai, Japan).
[16] Data sheet of Fuji Ceramics Cooperation (Sizuoka, Japan).
[17] Data sheet of NANOSENSORS Gmbh & Co. KG (D-35578, Wetzlar Blankenfeld, Germany).
[18] Y. H. Hu, M. C. Helen, X. W. Zhang, and M. P. Harmer, J. Am. Ceram. Soc. **69**, 549 (1986).
[19] A. Gruverman, O. Auciello, R. Ramesh, and H. Tokumoto, Nanotechnology **8**, A38 (1997).
[20] S. Hong, J. Woo, H. Shin, J. U. Jeon, Y. E. Pak, E. L. Colla, N. Setter, E. Kim, and K. No, J. Appl. Phys. **89**, 1377 (2001).
[21] In the UAFM experiment, because a small contact area cannot compensate the all polarization charge over the domain, the stiffness is probably enhanced by the piezoelectric stiffening effect (Ref. 26). Therefore, we use a stiffness coefficient at constant electric displacement c_{33}^D. It is given by substituting the stiffness coefficient at constant electric field c_{33}^E=62 GPa and the electromechanical coupling coefficient k_{33}=0.75 into Eq. 3 (Ref. 16). The result is c_{33}^D=117 GPa.
[22] K. L. Johnson, *Contact Mechanics* (Cambridge University Press, Cambridge, UK, 1985), Chap. 4.
[23] S. K. U. Kuno, *Micromechanics of Composites* (Hanser, New York, 1996), p. 15.
[24] Although this result is a relative comparison of the stiffness within the observation area, it will be calibrated by the additional UAFM experiment using the reference material such as single-crystal silicon. A detailed procedure was presented in Refs. 8 and 9.
[25] There is no conclusive opinion about the width of the DB in PZT because of the variety of the materials. As for $PbTiO_3$ that is prototypical material of the PZT, the width is attributed in the range of 1–5 nm at an epitaxial film and a single crystal (Refs. 5 and 7).
[26] T. Ikeda, *Fundamentals of Piezoelectricity* (Oxford University Press, New York, 2004), p. 27.